

# ANALYSIS OF THE DISCONTINUOUS PWM CONTROLLED D-STATCOM FOR REACTIVE POWER COMPENSATION APPLICATIONS

M. Mustafa Ertay, Ahmet Zengin

Original scientific paper

The scope of this paper covers the investigations of discontinuous PWM (DPWM) control of the Distribution Static Synchronous Compensator (D-STATCOM). Various DPWM methods have been widely used in motor drives for controlling the inverter and reducing power losses. With the rising demand for energy, energy efficiency has currently become an issue of vital importance. As a result, the use of the D-STATCOM in distribution systems is becoming increasingly common. In this study, DPWM methods were used for the D-STATCOM inner control. For the outer control, phase angle control was used and PWM methods were adapted to this control algorithm. In addition, conventional continuous PWM (CPWM) methods were applied to the D-STATCOM for comparison purposes. All simulations were performed in the MATLAB-Simulink software environment. Power losses have a significant impact on the D-STATCOM; therefore, a simulation model was developed to calculate the conduction and switching losses in order to investigate the effectiveness of DPWM methods in reducing the D-STATCOM power losses. Results showed that the utilization of different DPWM methods in the D-STATCOM was suitable for high modulation indexes. This clearly illustrates that, according to different DPWM methods, a reduction of from 14 % up to 50 % in D-STATCOM switching losses can be achieved. Furthermore, this study proposes the use of CPWM and DPWM methods in low and high modulation indexes, respectively, according to the requirements of the distribution system.

**Keywords:** continuous PWM (CPWM), discontinuous PWM (DPWM), distribution systems, D-STATCOM, phase angle control, power losses

## Analiza diskontinuiranog PWM kontroliranog D-STATCOM-a u primjenama kompenzacije reaktivne energije

Izvorni znanstveni članak

U ovom se radu opisuju istraživanja diskontinuirane PWM (DPWM) kontrole Distribucijskog Statičkog Sinkroniziranog Kompenzatora (D-STATCOM). Različite su se DPWM metode uveliko koristile u pogonskom sistemu motora za kontrolu invertora i smanjenje gubitaka energije. S povećanim potrebama za energijom, energetska učinkovitost postala je pitanje od osnovne važnosti. Rezultat toga je sve češća upotreba D-STATCOM-a u distribucijskim sustavima. U ovom su radu DPWM metode primijenjene za unutarnju kontrolu D-STATCOM-a. Za vanjsku je kontrolu korištena kontrola faznog ugla te su PWM metode prilagođene tom kontrolnom algoritmu. Uz to, na D-STATCOM primijenjene su uobičajene kontinuirane PWM (CPWM) metode u svrhu komparacije. Sve su simulacije provedene u okruženju MATLAB-Simulink softvera. Gubitci snage značajno utječu na D-STATCOM te je stoga razvijen simulacijski model za izračunavanje gubitaka provođenja i prekidanja u svrhu ispitivanja učinkovitosti DPWM metoda u reduciranju gubitaka snage D-STATCOM-a. Rezultati su pokazali da je primjena raznih DPWM metoda na D-STATCOM-u prikladna za indekse visoke modulacije. To jasno pokazuje da se, u skladu s različitim DPWM metodama, može postići smanjenje gubitaka od 14 % do 50 % pri uključivanju/isključivanju D-STATCOMa. Nadalje, u ovom se radu predlažu primjene metoda CPWM i DPWM kod niskih i visokih indeksa modulacije, prema potrebama distribucijskog sustava.

**Ključne riječi:** diskontinuirani PWM (DPWM), distribucijski sustavi, D-STATCOM, gubitci snage, kontrola faznog ugla, kontinuirani PWM (CPWM)

## 1 Introduction

The Distribution Static Compensator (D-STATCOM) is one of the converter-based custom power devices used for solving the problems of power quality and reactive power compensation in distribution power systems [1], [2]. At present, D-STATCOMs are increasingly being installed and used in distribution systems [2]. Generally, the power stage of the D-STATCOM consists of voltage source converters (VSCs), as seen in Fig.1 [1, 3]. The D-STATCOM generates three phase output voltages almost in phase with the ac network with which it is coupled through a coupling inductance [1, 3]. In addition it requires only a small dc capacitor in its VSC [1].

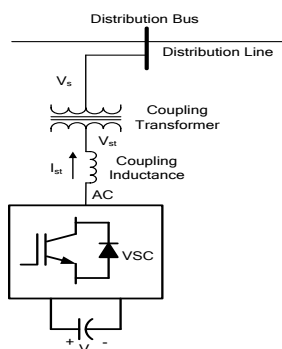


Figure 1 General configuration of D-STATCOM

In the literature there are several studies and investigations carried out in order to analyse the different viewpoints of D-STATCOM [2 ÷ 5].

An important part of the total losses of D-STATCOM are VSC losses [6]. In [1, 4] selective harmonic elimination method (SHEM) has been used for eliminating the two-level VSC harmonics of the D-STATCOM. The authors stated that switching losses were reduced by using the SHEM method due to the decrease of the switching frequency. Furthermore in [5, 6] SHEM method was applied to a STATCOM for the same purposes. In [7, 8] phase-shifted SPWM method has been used for multilevel converter configurations of STATCOMs. In [9, 10] the space vector PWM (SVPWM) method has been utilized for different power circuits and usage fields of STATCOMs, such as wind power. In [11] three converter structures (diode clamped, cascaded and hybrid converter) used in STATCOMs have been investigated against losses and different load conditions. In that study the SVPWM was used in STATCOMs. Furthermore, in [12] DPWM methods have been utilized in active power filters, and the authors of the study proposed a generalized DPWM strategy that reduced switching losses up to 46 % as compared to CPWM methods.

This paper focuses on the utilization of DPWM methods in D-STATCOMs in order to reduce the

switching losses and analyse the performance on reactive power compensation. For this purpose, a simulation model was developed to calculate the conduction and switching losses and the results obtained from the developed losses calculation model were reported. This model can also be used for calculating the IGBT losses in power electronics studies of dc-dc converters, multilevel inverters and rectifiers. In addition to utilizing DPWM methods, the reactive power compensation characteristic of the D-STATCOM was also reported in the present study. It was found that DPWM methods can be used for D-STATCOMs in high modulation range. Additionally, switching losses were reduced up to 50 % compared to CPWM methods.

**2 Description and operating principle of D-STATCOM**

A STATCOM utilized for a distribution system in a low to medium rating is called a D-STATCOM [13]. The D-STATCOM is connected in parallel with the ac system and composed of a VSC connected with a dc link capacitor, as seen in Fig. 1. The D-STATCOM is connected to the ac system by a coupling inductance and a coupling transformer. The D-STATCOM based on the implementation in distribution systems can be operated for the purposes given below [14]:

- a) Voltage control at a specific ac bus
- b) Reactive power compensation of a specific load
- c) Reactive power compensation and/or harmonic compensation of a specific load.

**3 Modelling of continuous and discontinuous PWM algorithms**

The PWM methods used in the inner control of the D-STATCOM were modelled in this section. These methods can be divided into two groups: continuous and discontinuous PWM methods.

The most important part of the D-STATCOM is the VSC. In Fig. 2, a diagram of a classic VSC is displayed [15]. Various PWM algorithms can be utilized in VSCs, depending on the desired application. This PWM algorithm was implemented by two methods: the triangle intersection method [15] and the direct digital technique [15, 16].

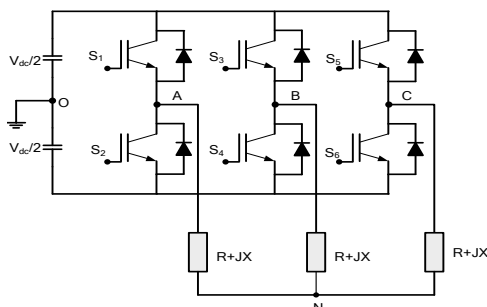


Figure 2 Power circuit of a three phase two level VSC

As can be seen in Fig. 2, the zero sequence signal ( $V_{ZSS}$ ) can be injected to the three reference modulation waves when utilizing the  $V_{NO}$  potential. When the  $V_{ZSS}$  is appropriately chosen, the linearity range of the PWM method can be extended. The  $V_{ZSS}$  can enhance the

waveform quality and reduce the switching losses of VSCs [15].

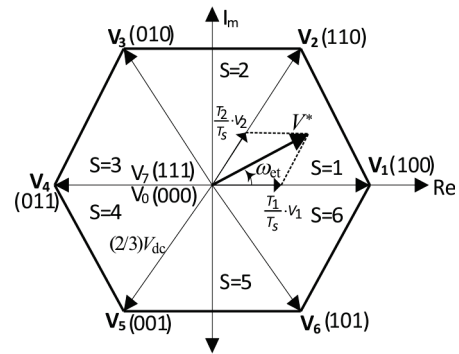


Figure 3 Space vector diagram of voltage space vectors

In the direct digital technique, the switching states of the VSC are calculated for each carrier cycle by using the space vector theory, as shown in Fig. 3 [15]. In two-level VSCs there are eight possible switching states; among these states there are six active and two zero state vectors (Fig. 3). In the SVPWM technique, by using the space vector theory seen in Fig. 3, reference voltages ( $V_{abc}$ ) are transformed into a complex reference voltage vector ( $V^*$ ), as in (1). In Eq. (1)  $a = e^{j(2\pi/3)}$  [15].

$$V^* = \frac{2}{3} (V_a^* + a \cdot V_b^* + a^2 V_c^*) = V_{1m}^* \cdot e^{j\omega_{et}} \tag{1}$$

In (1)  $V_{1m}$  is the first sector voltage vector and the  $V^*$  voltage rotates with  $\omega_{et}$  angle [15, 17]. The time lengths of VSC state vectors can be calculated as in Eq. (2) by using Figs. 3 and 4 [17]:

$$\begin{aligned} T_a &= k_0 T_0 + T_2 + T_1, \\ T_b &= k_0 T_0 + T_2, \\ T_c &= k_0 T_0, \end{aligned} \tag{2}$$

where  $T_a$ ,  $T_b$  and  $T_c$  are the durations of switching pulses of  $S_1$ ,  $S_3$  and  $S_5$  switches, respectively [17]. In Eq. (2)  $k_0$  is a factor between  $0 \leq k_0 \leq 1$ . It defines the timing of zero vectors. The SVPWM modulation waves can be obtained by adding a  $V_{ZSS}$  signal to the reference voltages as in Eq. (3) [17]. The  $V_{ZSS}$  signal of SVPWM can be obtained by using Eq. (4) [17].

$$V_{abc}^{**} = V_{abc}^* + V_{ZSS}, \tag{3}$$

$$V_{ZSS} = -\left[ (1-2k_0) - k_0 V_a^* + (1-k_0) V_c^* \right]. \tag{4}$$

The DPWM was first developed and proposed by Depenbrock [18], in 1977. The basic idea underlying the DPWM method is reduction of the switching number in every switching cycle. Therefore, one phase is clamped to positive ( $+V_{dc}/2$ ) or negative ( $-V_{dc}/2$ ) dc bus for 1/3 of the switching period. During this time period, modulation is provided by the other two phases. It can be clearly seen that there are no switching losses during the corresponding clamped phase in this time period. Hence, total switching losses can be reduced, theoretically an average of 33 %, as

compared to CPWM methods [12, 15, 16, 17, 19, 20].

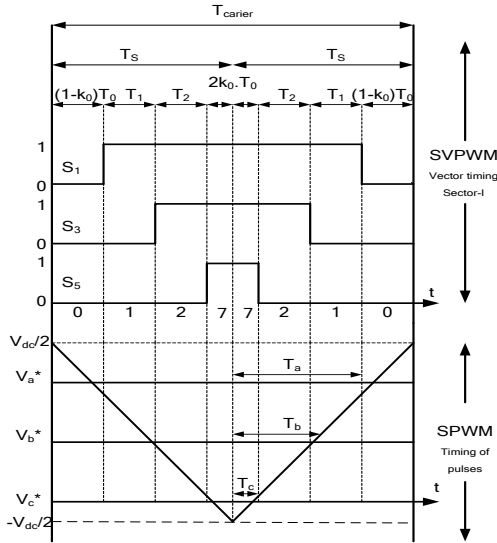


Figure 4 VSC switching states for one carrier cycle in SVPWM and SPWM

Although there are several studies dealing with the application and investigation of DPWMs in various fields of power electronics [12, 15, 16, 17, 19, 20], no paper has been found in the literature that investigates the effects of DPWM methods on the D-STATCOM. There are many DPWM algorithms in the literature. According to the distribution of zero vectors and different shapes of  $V_{ZSS}$  signals, different DPWM modulation waves can be generated by using the method given in [17]. Using Eqs. (3) and (4), the  $V_{ZSS}$  of different DPWM methods can be obtained by varying the  $k_0$  factor in Eq. (5) [17].

$$V_{ZSS} = -[(1 - 2k_0) - k_0V_{max}^* + (1 - k_0)V_{min}^*], \quad (5)$$

$$V_{ZSS} = -0,5(V_{max}^* + V_{min}^*) = 0,5V_{mid}^*, \quad (k_0 = 0,5).$$

In Eq. (5)  $V_{max}^*$ ,  $V_{min}^*$  and  $V_{mid}^*$  are the maximum, minimum and middle values of the original input reference voltages [17]. By using Eq. (5) one can obtain modulation waveforms of DPWM methods in MATLAB-Simulink, as shown in Fig. 5.

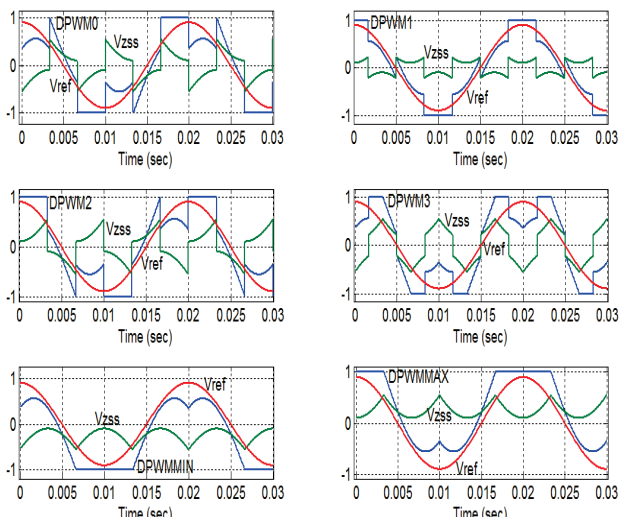


Figure 5 Modulation waveforms of DPWM methods with voltage reference and zero sequence signals ( $M=0,9$ )

#### 4 Calculation of switching and conduction losses of D-STATCOM

The switching losses of a VSC depend on the D-STATCOM current magnitude and dc link voltage. The switching energy of VSC switches is divided into turn-on energy ( $E_{ON}$ ) and turn-off energy ( $E_{OFF}$ ) [21]. The switching energy losses of a VSC switch can be defined as linear functions of the collector current and the dc link voltage by Eqs. (6) and (7) [4, 21]:

$$E_{ON} = E_{on} \cdot \frac{I_C}{I_{Cnom}} \cdot \frac{V_{CC}}{V_{CCnom}}, \quad (6)$$

$$E_{OFF} = E_{off} \cdot \frac{I_C}{I_{Cnom}} \cdot \frac{V_{CC}}{V_{CCnom}}, \quad (7)$$

where  $I_C$  and  $V_{CC}$  values are the actual D-STATCOM IGBT collector current and the dc voltage of the IGBT, respectively [4, 21]. The  $I_{Cnom}$  and  $V_{CCnom}$  values are the reference values of the IGBT collector current and dc voltage obtained from the datasheet of IGBTs [22]. The  $E_{on}$  and  $E_{off}$  values are switching energies per pulse. These are also obtained from the datasheet. For a realistic calculation of switching and conduction losses, the high-power IGBT product CM1500HC-66R, which can be used at a medium voltage level, was selected. The data sheet of this product is available on the Mitsubishi Corporation web site [22]. The switching power losses of the D-STATCOM can be calculated by using Eqs. (8) and (9) [4, 21]:

$$P_{SWON} = f_{SW} \cdot \sum_{i=1}^n \left[ E_{on} \cdot \frac{I_C}{I_{Cnom}} \cdot \frac{V_{CC}}{V_{CCnom}} \right], \quad (8)$$

$$P_{SWOFF} = f_{SW} \cdot \sum_{i=1}^n \left[ E_{off} \cdot \frac{I_C}{I_{Cnom}} \cdot \frac{V_{CC}}{V_{CCnom}} \right], \quad (9)$$

where  $n$  and  $f_{SW}$  are the number of pulses in the switching period and switching frequency, respectively [4, 21]. In Fig. 6, one phase leg of a two-level VSC is shown. During operation, if the  $D_1$  diode is on, its opposite IGBT  $S_1$  is off. Similarly, if  $S_1$  is on,  $D_2$  conducts when the  $S_1$  turns off [21, 23]. It is clear that only one switch is on at any single switching time.

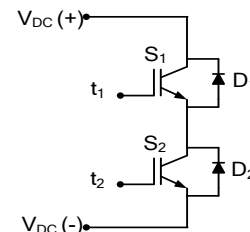


Figure 6 One phase leg of VSC

The switching losses of the diodes ( $D_1$  and  $D_2$ ) are reverse recovery losses; actually corresponding to the turn-off energy loss per pulse and can be calculated as in Eq. (10) [21, 23]:

$$P_{SWD} = f_{SW} \cdot \sum_{i=1}^n \left[ E_{rre} \cdot \frac{I_C}{I_{Cnom}} \cdot \frac{V_{CC}}{V_{CCnom}} \right] \tag{10}$$

If we normalize the switching losses of the D-STATCOM under DPWM methods to the switching losses of the D-STATCOM under CPWM methods, the switching loss factor (SLF) is obtained. It can be calculated as in Eq. (11) [12, 15, 19, 20]:

$$SLF = \frac{P_{SWDPWM}}{P_{SWCPWM}} \tag{11}$$

It is clear that, depending on the different DPWM methods, the SLF is varied according to the current phase angle [12]. The conduction losses of the VSC switches are calculated as in Eq. (12) [16, 21 ÷ 23]:

$$P_{CON} = \frac{1}{T} \cdot \left( \sum_{i=1}^n \int_{t_0}^{t_1} V_{CE} \cdot I_C dt \right) + I_{CRMS}^2 \cdot R_D \tag{12}$$

where  $V_{CE}$ ,  $I_{CRMS}$ ,  $R_D$  and  $T$  are the collector emitter saturation voltage of the IGBT, the RMS value of the collector current, the dynamic resistance of the IGBT, and the switching period, respectively [16, 21 ÷ 23]. In this study, the  $V_{CE}$  and  $R_D$  were determined from the datasheet [22]. The  $R_D$  value was calculated for  $T_J = 125^\circ\text{C}$ , from the

graphic of collector-emitter saturation voltage characteristics and, depicted in the datasheet of the IGBT [22]. The conduction losses of the diodes can be calculated as in Eq. (13) [21 ÷ 23]:

$$P_{COND} = \frac{1}{T} \cdot \left( \sum_{i=1}^n \int_{t_0}^{t_1} V_{EC} \cdot I_C dt \right) + I_{CRMS}^2 \cdot R_{DD} \tag{13}$$

where  $V_{EC}$  is the emitter-collector voltage of the diode and  $R_{DD}$  is the dynamic resistance of the diode that is calculated from the freewheel diode forward characteristics in the datasheet [22].

### 6 The phase angle control method of D-STATCOM

The phase angle control method was used in the outer control of the D-STATCOM [1]. In this control technique, the angle  $\delta$  between the system voltage  $V_s$  and the D-STATCOM voltage  $V_{st}$  changes when for accomplishing the reactive power compensation while the modulation index is kept constant. Therefore, to control the D-STATCOM output voltage, the dc link voltage is permitted to change. The phase angle control scheme of the D-STATCOM is shown in Fig. 7. To change the amount of reactive power absorbed or delivered by the D-STATCOM DC link voltage ( $V_{DC}$ ) must be set by the control of  $\delta$  [3]. In Fig. 7, the phase angle is controlled by the PI controller.

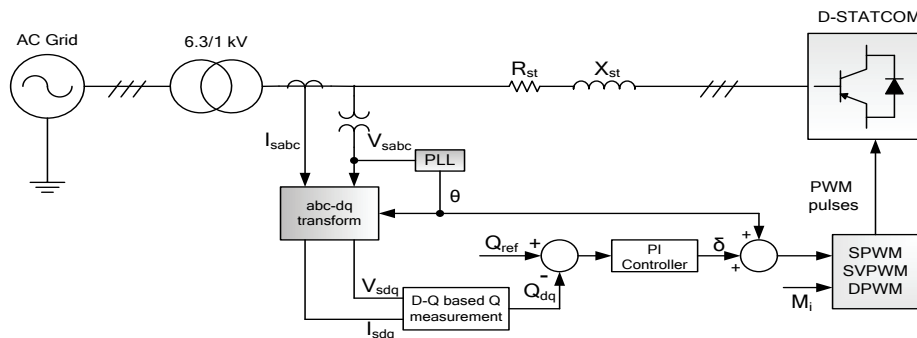


Figure 7 The principle scheme of the phase angle control of the D-STATCOM

As shown in Fig. 7, the reactive power error was applied to the PI controller. The output of the PI controller is  $\delta$ , the phase angle of modulation signals. In this scheme,  $M_i$  is the modulation index, which is the amplitude of the modulation signals that is kept constant. Three phase-abc modulation signals obtained from this scheme were  $M_i \sin(\delta + \theta)$ ,  $M_i \sin(\delta + \theta - 2\pi/3)$  and  $M_i \sin(\delta + \theta + 2\pi/3)$ , respectively [3].

### 5 Modeling and control of the D-STATCOM System in Matlab-Simulink

For this study, the D-STATCOM system which is depicted in Fig. 8 was modeled in a MATLAB-Simulink environment and shows the single line diagram of the system. The coupling inductance resistance and the reactance of the D-STATCOM are  $R_{st}$  and  $X_{st}$ , respectively. The primary objective of the D-STATCOM in this system was the reactive power compensation of a  $P \pm jQ$  (300 kW  $\pm$  j250 kvar) load. The power factor of the system without

the D-STATCOM was 0,7682 leading/lagging. The D-STATCOM was under unity power factor operation. The general view of the D-STATCOM system in MATLAB-Simulink is illustrated in Fig. 9.

The obtained IGBT current wave shape is shown in Fig. 10. As can be seen in these figures, the time intervals  $t = 0,516$  s to  $t = 0,536$  s, in which the D-STATCOM operation was in a steady state, were selected. The power losses were calculated for this period of simulation time. In Fig. 11 and 12, the collector current and IGBT voltage signals related to the DPWM2 method are shown.

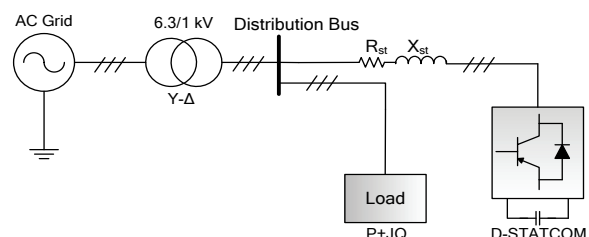


Figure 8 The D-STATCOM system under study

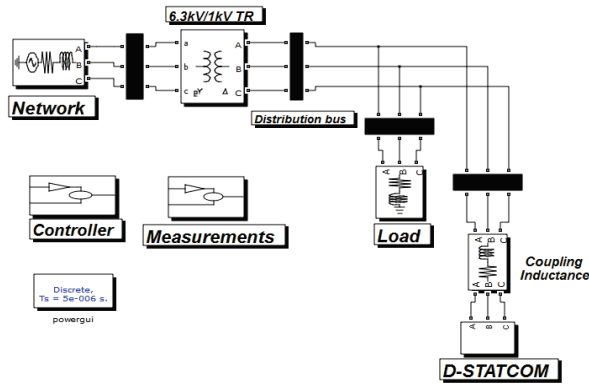


Figure 9 General view of the D-STATCOM system in Matlab-Simulink

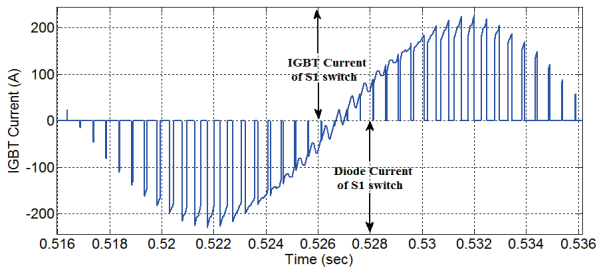


Figure 10 The IGBT current signal of  $S_1$  switch while D-STATCOM is in capacitive mode of operation (Generating 250 kVAR capacitive reactive power with SPWM method with  $M_i = 0,94$ )

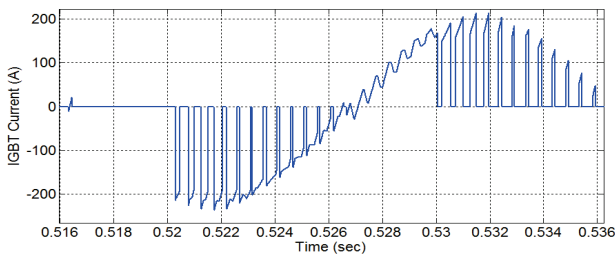


Figure 11 The IGBT current signal of  $S_1$  switch while D-STATCOM is in capacitive mode of operation (Generating 250 kVAR capacitive reactive power with DPWM2 method with  $M_i = 0,94$ )

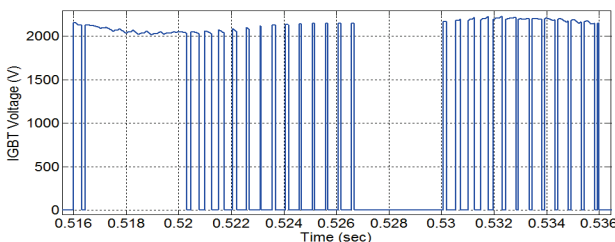


Figure 12 The IGBT voltage signal of  $S_1$  switch while D-STATCOM is in capacitive mode of operation with DPWM2

## 7 The simulation results and discussion

For analysing the performance of DPWM methods on controlling the D-STATCOM, several simulations were carried out. In these simulations, first, for the capacitive and inductive operation of the D-STATCOM, the voltage and current harmonics of the system, power losses of the D-STATCOM and dc link voltage were calculated and analysed for  $M_i = 0,94$ . Second, by changing the  $M_i$  and switching frequency of the D-STATCOM, analyses of the voltage and current harmonics of the system, power losses of the D-STATCOM and the dc link voltage were performed according to the capacitive and inductive operation modes of the D-STATCOM.

In Fig.13, the variations in reactive power in DB (in capacitive mode when  $M_i = 0,94$ ) when using the SPWM method can be seen. In Figs. 14 and 15, the results of reactive power compensation in DB when using DPWMMIN and DPWMMAX are illustrated. These methods have shown good performances in reactive power compensation in terms of stability. It is clearly shown in Figs. 16 and 17 that when the modulation index is increased, the stability of the reactive power compensation is increased as well while using the DPWM3 method in capacitive operation mode. Figs. 18 ÷ 21 illustrate the phase to dc bus midpoint voltage of the D-STATCOM with  $M_i = 0,94$ , in capacitive operation mode when using the DPWM0, DPWM1, DPWM2 and DPWM3 methods, respectively. As seen in Figs. 18 ÷ 21, the VSC phase legs are clamped to the dc bus according to their clamping degrees in the DPWM methods.

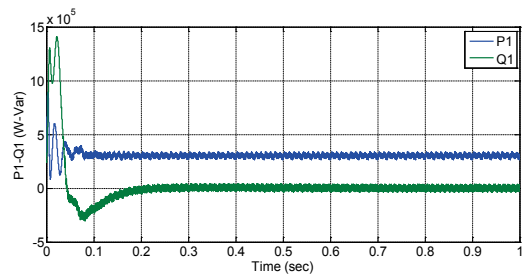


Figure 13 Control of reactive power of DB and variation of active power in DB when SPWM method is used ( $M_i = 0,94$ )

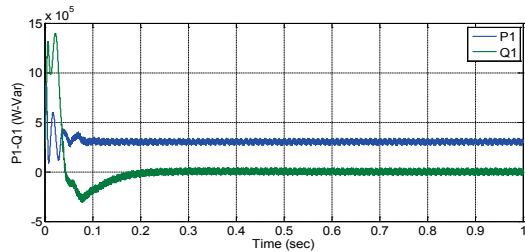


Figure 14 Control of reactive power of DB and variation of active power in DB when DPWMMIN method is used (in capacitive mode,  $M_i = 0,94$ )

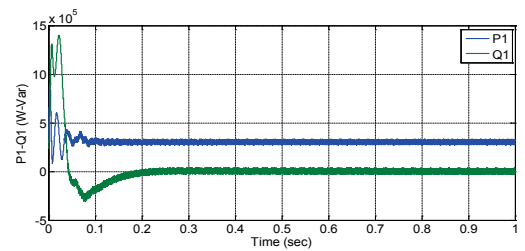


Figure 15 Control of reactive power of DB and variation of active power in DB when DPWMMAX method is used (in capacitive mode,  $M_i = 0,94$ )

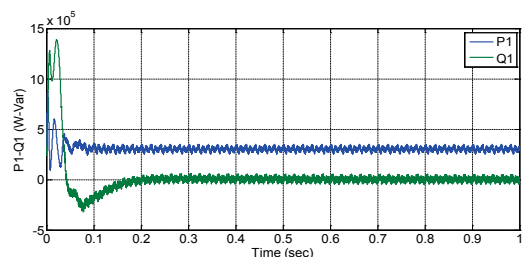
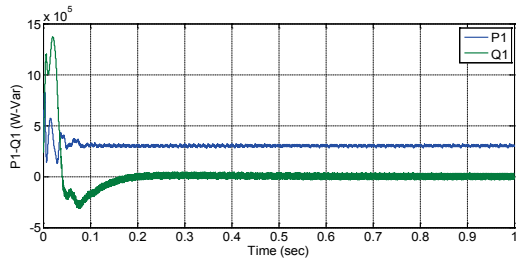
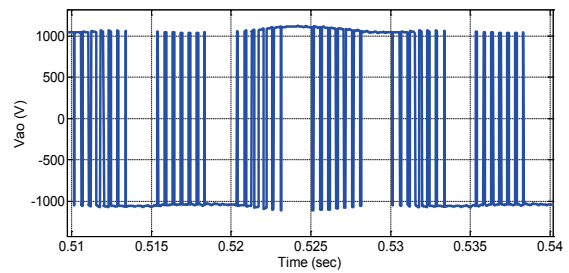


Figure 16 Control of reactive power of DB and variation of active power in DB when DPWM3 method is used (in capacitive mode,  $M_i = 1$ )



**Figure 17** Control of reactive power of DB and variation of active power in DB when DPWM3 method is used (in capacitive mode,  $M_i=1,15$ )



**Figure 21** Phase voltage of D-STATCOM in capacitive operation mode when DPWM3 method is used ( $M_i=0,94$ )

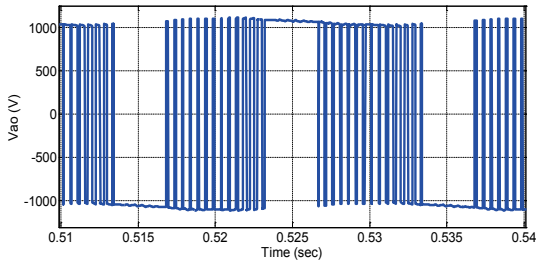


**Figure 18** Phase voltage of D-STATCOM in capacitive operation mode when DPWM0 method is used ( $M_i=0,94$ )

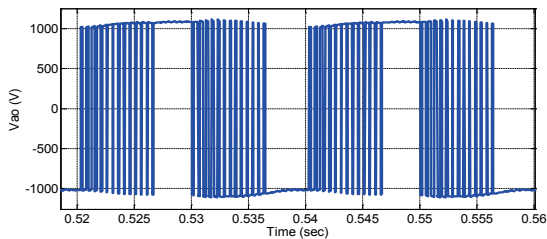


**Figure 19** Phase voltage of D-STATCOM when DPWM1 method is used in capacitive operation mode ( $M_i=0,94$ )

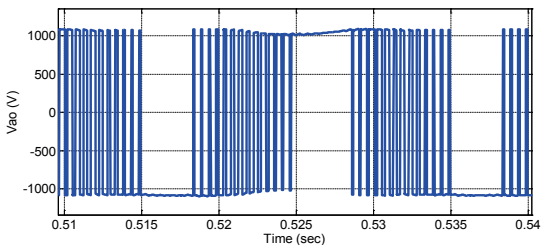


**Figure 20** Phase voltage of D-STATCOM in capacitive operation mode when DPWM2 method is used ( $M_i=0,94$ )

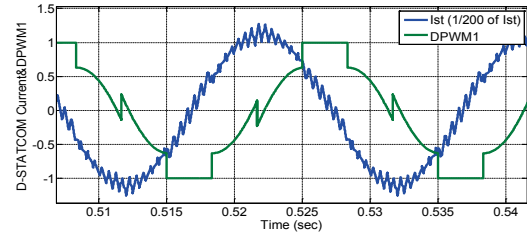


**Figure 22** Variation of D-STATCOM current against modulation wave of DPWM1 in capacitive operation mode ( $M_i=0,94$ )

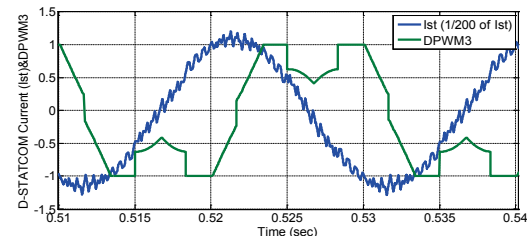


**Figure 23** Variation of D-STATCOM current against modulation wave of DPWM3 in capacitive operation mode ( $M_i=0,94$ )

In Figs. 22 and 23, the modulation waves of DPWM1 and DPWM3, respectively, are shown against the 1/200 of D-STATCOM current. In Tab. 1, one can see that the DPWM3 method was superior to the other DPWM methods in this system, as the DPWM3 had SLFs of 51,2 % and 49,58 % in capacitive and inductive operation modes of the D-STATCOM, respectively. This means that switching losses were reduced by 48,80 % and 50,42 % in capacitive and inductive operation modes, respectively, when compared to the SPWM method.

**Table 1** Investigation of power losses of D-STATCOM against PWM Methods ( $M_i=0,94, F_{sw}=2\text{ kHz}$ )

PWM Method	D-STATCOM Operation	Power losses (W)			SLF (%)		Reduction (%)	
		Switching	Conduction	Total	SPWM	SVPWM	SPWM	SVPWM
SPWM	Capacitive	596,4	854,7	1451	-	-	-	-
	Inductive	602	852,3	1454	-	-	-	-
SVPWM	Capacitive	573,2	827,7	1401	96,10	-	3,9	-
	Inductive	585,7	842,8	1428	97,29	-	2,71	-
DPWM0	Capacitive	462,6	836	1299	72,56	80,70	27,44	19,30
	Inductive	403,3	836,8	1240	66,99	68,85	33,11	31,15
DPWM1	Capacitive	479,7	767	1247	80,43	83,68	19,57	16,32
	Inductive	502,4	824,4	1327	83,45	85,77	16,55	14,23
DPWM2	Capacitive	388,5	852,9	1241	65,14	67,77	34,86	32,23
	Inductive	467,6	848,8	1316	77,67	79,83	22,33	20,17
DPWM3	Capacitive	305,4	877	1182	51,20	53,27	48,80	46,73
	Inductive	298,5	843,5	1142	49,58	50,96	50,42	49,04
DPWMMIN	Capacitive	411,3	821	1232	68,96	71,75	31,04	29,25
	Inductive	408,3	838,6	1247	67,82	69,71	32,18	30,29
DPWMMAX	Capacitive	425	820,5	1245	71,26	74,14	28,74	25,86
	Inductive	419,9	833,7	1254	69,75	71,69	30,25	28,31

When the SVPWM was considered, the DPWM3 had SLFs of 53,27 % and 50,96 % in capacitive and inductive operation modes of the D-STATCOM, respectively. The DPWM3 was superior to the other DPWM methods because the clamping was performed in higher values of D-STATCOM current than the other DPWM methods, as seen in Fig. 23. In contrast, the DPWM1 method showed the worst performance when considering SLF values both in capacitive and inductive operation modes, since these were 80,43 % and 83,45 %, respectively. This means there was a reduction of 19,57 % and 16,55 % in switching losses in capacitive and inductive operation mode, respectively, against the SPWM method. When the SVPWM was considered, the DPWM1 had SLFs of 83,68 % and 85,77 % in capacitive and inductive operation modes respectively. The DPWM1 resulted in lower reduction than the other DPWM methods because the clamping was performed in the lower values of the D-STATCOM current, as seen in Fig. 22. As mentioned above, switching losses are proportional to switch current and voltage. The results for the other DPWM methods can be seen in Tab. 1: DPWM0, DPWM2, DPWMMIN and DPWMMAX methods had good performances in terms of switching loss reduction; approximate values are obtained.

The SPWM and SVPWM methods exhibited good performances in DB harmonic current values in both low and high modulation indexes in the inductive mode of operation (Fig. 24). Considering the DPWM methods, harmonic current values are high in low modulation indexes, especially after  $M_i = 1$ , they performed well in terms of harmonic distortion, especially after  $M_i = 1$ , they performed well in terms of harmonic distortion. For  $M_i = 1,155$ , DPWM3 had a performance superior to the other PWM methods in terms of harmonic current values (Fig. 24). A similar statement can be made for capacitive operation (Fig. 25). In Fig. 26 ÷ 27, the changing of the harmonic current values of the D-STATCOM against the changing of the modulation index is demonstrated: the DPWM3 had lower harmonic values in both capacitive and inductive operations in the modulation index of  $M_i = 1,155$ .

In Fig. 28, the switching losses of the D-STATCOM against the variation of frequency for the PWM methods are shown for the inductive operation mode. Clearly, if the frequency is increased, the difference between the DPWM methods and the CPWM methods increases due to the reduction of switching losses. Moreover, it can be seen from Fig. 29 that the DPWM3 is superior to the other DPWM methods in terms of reduction of total losses. A reduction of 52,2 % was achieved in total losses when utilizing DPWM3 in a 10 kHz case. In Fig. 30, the variations of switching losses of the D-STATCOM against the variations of frequency for the PWM methods are given for the capacitive operation mode. Here it is obvious that the DPWM3 is superior to the other DPWM methods in terms of reduction of switching losses. A reduction of 56,8 % in switching losses was achieved when utilizing the DPWM3 in the 10 kHz case. In Fig. 31, the variation of total losses of the D-STATCOM against the variation of frequency for PWM methods for the capacitive operation mode is shown. A reduction of 48,2 % in total losses was achieved when utilizing the DPWM3 in the 10 kHz case.

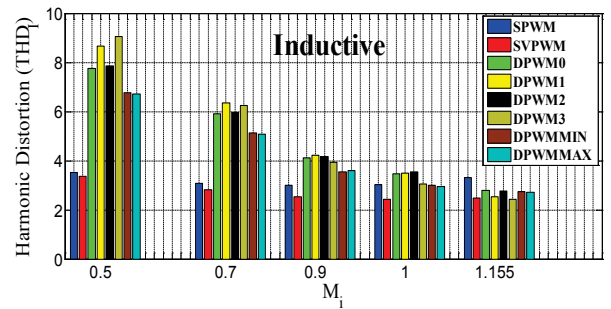


Figure 24 Changing of harmonic current values of DB against changing of modulation index for PWM methods (Inductive operation,  $f_{sw} = 2$  kHz)

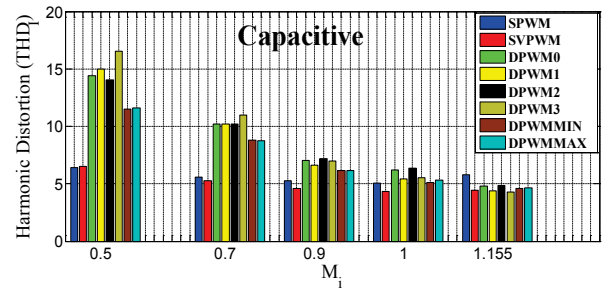


Figure 25 Changing of harmonic current values of DB against changing of modulation index for PWM methods (Capacitive operation,  $f_{sw} = 2$  kHz).

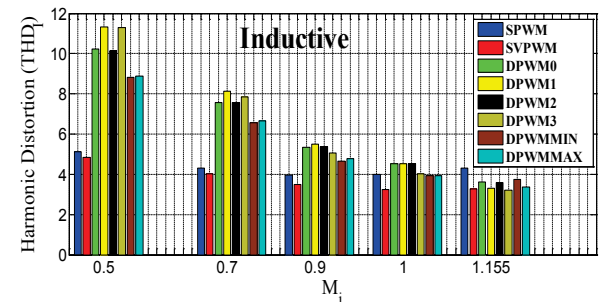


Figure 26 Harmonic current values of D-STATCOM against changing of modulation index for PWM methods (Inductive operation,  $f_{sw} = 2$  kHz)

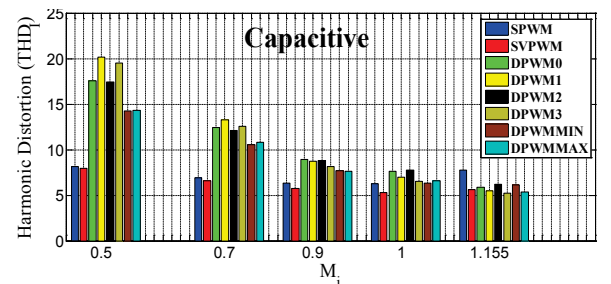


Figure 27 Changing of harmonic current values of D-STATCOM against changing of modulation index for PWM methods (Capacitive operation,  $f_{sw} = 2$  kHz)

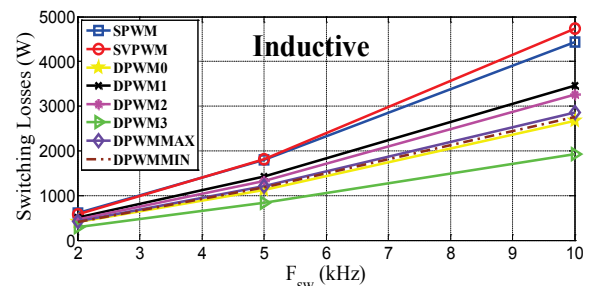


Figure 28 Changing of switching losses of D-STATCOM against changing of frequency for PWM methods (Inductive operation,  $M_i = 0,94$ )

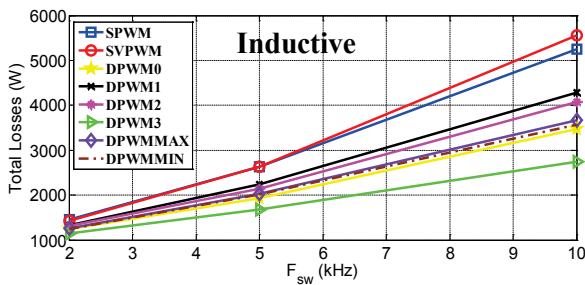


Figure 29 Changing of total losses of D-STATCOM against changing of frequency for PWM methods (Inductive operation,  $M_i = 0,94$ )

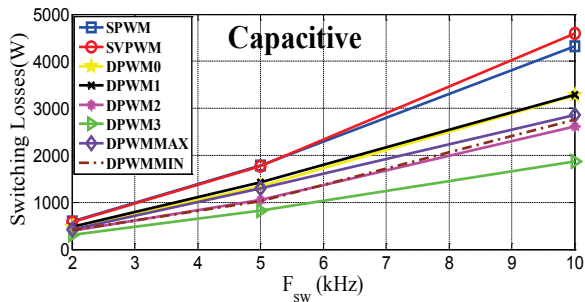


Figure 30 Changing of switching losses of D-STATCOM against changing of frequency for PWM methods (Capacitive operation,  $M_i = 0,94$ )

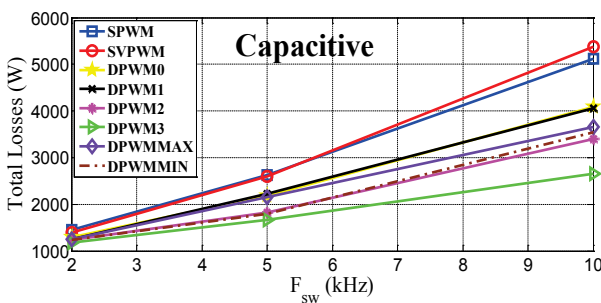


Figure 31 Changing of total losses of D-STATCOM against changing of frequency for PWM methods (Capacitive operation,  $M_i = 0,94$ )

## 8 Conclusions

In this paper, the use of DPWM methods in the D-STATCOM was investigated for reactive power applications. After the results were reported, it was found that the DPWM3 method was the best in switching losses reduction compared to the other DPWM methods in the D-STATCOM. A reduction from 14 % up to 50 % can be achieved with the utilization of DPWM methods as compared to CPWM methods. The load power factor is obviously also an important parameter in choosing the suitable DPWM method to be utilized in the D-STATCOMs. In general, these results indicate that DPWM methods can be applied to D-STATCOMs for high modulation indexes, especially after the modulation index of 1. Furthermore, the results show that current harmonic distortions obtained in the D-STATCOM for the low modulation indexes with the utilization of DPWMMAX and DPWMMIN methods were lower than the other DPWM methods. As was mentioned earlier, utilization of these methods results in unequal stress in the semiconductor switches. Therefore, these two methods are not usually preferred or are limited in industrial applications. This paper proposes the utilization of the SPWM and SVPWM methods for low modulation

indexes, while DPWM methods are recommended for high modulation indexes. The proper PWM algorithm can be selected according to the requirements of the distribution system. It was found that the DPWM3 method seemed especially suitable for the reduction of switching losses and reactive power compensation in the D-STATCOM. It was also deduced from the results that this DPWM3 method demonstrated a good performance in terms of current harmonic distortion for high modulation indexes of the D-STATCOM.

## 9 References

- [1] Çetin, A.; Ermis, M. VSC-Based D-STATCOM With Selective Harmonic Elimination. // IEEE Trans. On Ind. Applications. 45, 3(2009), pp. 1000-1015.
- [2] Du, S., Liu, J. Study on DC Voltage Control for Chopper-Cell-Based Modular Multilevel Converters in D-STATCOM Application. // IEEE Trans. On Power Delivery. 28, 4(2013), pp. 2030-2038.
- [3] Coteli, R.; Deniz, E.; Dandil, B.; Tuncer, S.; Ata, F. Phase Angle Control of Three Level Inverter Based D-STATCOM Using Neuro-Fuzzy Controller. // Advances in Electrical and Computer Eng. 12, 1(2012), pp. 77-84.
- [4] Cetin, A. Design and Implementation of a Voltage Source Converter Based STATCOM for Reactive Power Compensation and Harmonic Filtering, PhD. Thesis, The Grad. School of METU, Ankara, 2007.
- [5] Filizadeh, S.; Gole, A. M. Harmonic Performance Analysis of an OPWM-Controlled STATCOM in Network Application. // IEEE Trans. on Power Delivery. 20, 2(2005), pp. 1001-1008.
- [6] Hingorani, N. G.; Gyugyi, L. Understanding FACTS: concepts and technology of flexible ac transmission systems. // IEEE Press. New York, 1999.
- [7] Sundararaju, K.; Nirmal Kumar A. Control Analysis of STATCOM with Enhanced Methods for Compensation of Load Variation. // European Journal of Scientific Research. 53, 4(2011), pp. 590-597.
- [8] Masdi, H.; Mariun, N.; Bashi, S. M.; Mohamed, A.; Yusuf S. Construction of a Prototype D-Statcom for Voltage Sag Mitigation. // European Journal of Scientific Research. 30 1(2009), pp. 112-127.
- [9] Shu, Z.; Ding, N.; Chen, J.; Zhu, H.; He, X. Multilevel SVPWM with DC-Link Capacitor Voltage Balancing Control for Diode-Clamped Multilevel Converter based STATCOM. // IEEE Trans. on Ind. Electronics, Issue: 99, 60, 5(2013), pp. 1884-1896.
- [10] Saeedifard, M.; Irvani, R.; Pou, J. Control and DC-capacitor voltage balancing of a space vector-modulated five-level STATCOM. // IET Power Electronics. 2, 3(2009), pp. 203-215.
- [11] Lauttamus, P.; Tuusa, H. Comparison of Five-Level Voltage-Source Inverter Based STATCOMs, Power Conversion Conference / Nagoya, 2007, pp. 659-666.
- [12] Asiminoaei, L.; Rodriguez, P.; Blaabjerg, F. Application of Discontinuous PWM Modulation in Active Power Filters. // IEEE Trans. on Power Electronics. 23, 4(2008), pp. 1692-1706.
- [13] Singh, B.; Saha, R.; Chandra, A.; Al-Haddad, K. Static synchronous compensators (STATCOM): a review. // IET Power Electron. 2, 4(2009), pp. 297-324.
- [14] Ledwich, G.; Ghosh, A. A flexible D-STATCOM operating in voltage or current control mode // IEE Proc. Gen. Tran. Distrib. 149, 2(2002), pp. 215-224.
- [15] Hava, A. M.; Kerkman, R. J.; Lipo, T. A. Simple and Analytical and Graphical Methods for Carrier-Based PWM-VSI Drives. // IEEE Trans. on Power Electronics. 14,



- 1(1999), pp. 49-60.
- [16] Wu, Y.; Shafi, M. A.; Knight, A. M.; McMahon, R. A. Comparison of the Effects of Continuous and Discontinuous PWM Schemes on Power Losses of Voltage-Sourced Inverters for Induction Motor Drives. // IEEE Tran. On Power Elec. 26, 1(2011), pp. 182-191.
- [17] Blasko, V. Analysis of a hybrid PWM based on modified space-vector and triangle-comparison methods. // IEEE Trans. on Industry Appl., 33, 3(1997), pp. 756-764.
- [18] Depenbrock, M. Pulse width control of a 3-phase inverter with non-sinusoidal phase voltages. // IEEE Int. Semiconductor Power Con. Conf., 1977, pp. 399-403.
- [19] Hava, A. M.; Kerkman, R. J.; Lipo, T. A. A high performance generalized discontinuous PWM algorithm. // IEEE Trans. Ind. Appl. 34, 5(1998), pp. 1059-1071.
- [20] Holmes, D. G.; Lipo, T. A. Pulse width Modulation for power Converters: Principles and Practice, IEEE Series on Power Eng., John Wiley & Sons, 2003.
- [21] Ivakhno, V.; Zamaruiev, V.; Ilina, O. Estimation of Semiconductor Switching Losses under Hard Switching using Matlab/Simulink Subsystem. // Electrical, Control and Commun. Eng. 2, 1(2013), pp. 20-26.
- [22] Datasheet of CM1500HC-66R, Mitsubishi Electric Corporation, URL://www.mitsubishielectric-mesh.com/products/pdf/cm1500hc-66r\_e.pdf, (10.07.2013).
- [23] Oberdorf, M. C. Power Losses And Thermal Modeling Of A Voltage Source Inverter, Naval Postgraduate School Monterey, California, Master Thesis, 2006.

#### Authors' addresses

***M. Mustafa Ertay, PhD Candidate, Research Assistant***

Duzce University  
Faculty of Technology  
Department of Electrical and Electronics Engineering  
Konuralp Campus, 81620, Duzce, Turkey  
E-mail: mustafaertay@duzce.edu.tr

***Ahmet Zengin, Assoc. Prof. Dr.***

Sakarya University  
Faculty of Technology  
Department of Computer Engineering  
Esentepe Campus, 54187, Sakarya, Turkey  
E-mail: azengin@sakarya.edu.tr